



ELSEVIER

Available online at www.sciencedirect.com

SCIENCE @ DIRECT®

Nuclear Instruments and Methods in Physics Research B 204 (2003) 705–719

NIM B
Beam Interactions
with Materials & Atoms

www.elsevier.com/locate/nimb

“Isotope language” of the Alpine Iceman investigated with AMS and MS

Walter Kutschera^{a,*}, Wolfgang Müller^{b,c}

^a Vienna Environmental Research Accelerator, Institute for Isotope Research and Nuclear Physics, University of Vienna, Währinger Strasse 17, A-1090 Vienna, Austria

^b Research School of Earth Sciences, The Australian National University, Canberra ACT 0200, Australia

^c Department of Earth Sciences, ETH Zürich, CH-8092 Zürich, Switzerland

Abstract

This paper reviews the use of stable and radioactive isotopes to elucidate an extraordinary archaeological find, the Alpine Iceman “Ötzi”. In 1991 the body of this man was accidentally discovered in an ice-filled depression at a high-altitude mountain pass (Tisenjoch, 3210 m) of the Ötztal Alps. This location at the Austrian–Italian border apparently formed an ancient transition across the Alps from South to North.

¹⁴C dating of the body with accelerator mass spectrometry (AMS) revealed that the Iceman had lived some 5200 years ago, within the time period from 3370 to 3100 years BC (Before Christ). A variety of other materials from the discovery site were also dated with ¹⁴C AMS suggesting a use of the mountain pass at other time periods, and varying climatic conditions.

Ongoing investigations with thermal ionization (TIMS), inductively-coupled plasma (ICP-MS) and gas mass spectrometry include isotope ratios of ¹⁸O/¹⁶O ($\delta^{18}\text{O}$), ⁸⁷Sr/⁸⁶Sr and ²⁰⁶Pb/²⁰⁴Pb, in order to reveal the Iceman’s origin and migrational behavior. Analyzed samples include tooth enamel, bones and contents of his intestine, which all represent different ontogenetic (developmental) stages. The isotopic composition of the Iceman is compared to both soils from archaeological sites and local waters. Taken together, the results point towards an origin of the Iceman in the Southeast of the finding site, consistent with archaeological and paleobotanical data.

© 2003 Elsevier Science B.V. All rights reserved.

Keywords: Radiocarbon, AMS; Dating of human and botanical remains, climate variation; Stable and radiogenic isotopes, MC-ICPMS, TIMS; Tracing of human origin

1. Introduction

Exceptional discoveries cannot be predicted. This truism in almost any field of human endeavor

was confirmed by the discovery of the Iceman high up in the glacial region of the Ötztal Alps, which happened on 19 September 1991. Two mountain hikers from Nürnberg, Erika and Helmut Simon, after having scaled the Finail Peak (3516 m) in the Ötztal Alps in Austria were on their way back to the Similaun lodge (3017 m) located at the lowest part of a mountain ridge connecting the Finail Peak with the Similaun Peak (Fig. 1). This ridge

* Corresponding author. Tel.: +43-1-4277-51701/51700; fax: +43-1-4277-9517.

E-mail address: walter.kutschera@univie.ac.at (W. Kutschera).

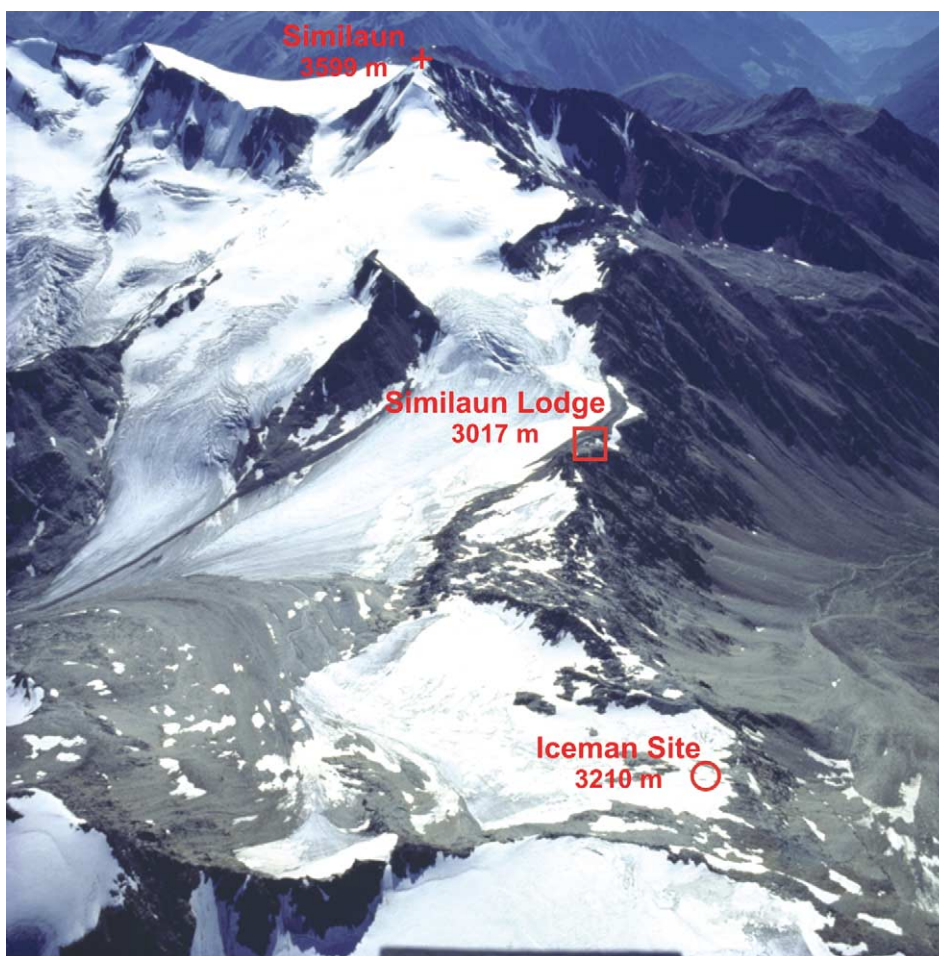


Fig. 1. Airphoto of the mountain range next to the Iceman site, located on the ridge running east towards the Similaun peak. The photo was taken on 21 August 1989 by Gernot Patzelt from the Institute of High Mountain Research of the University of Innsbruck, two years before the Iceman was discovered. The glaciers to the north (left) lead to the Ötztal in Austria, whereas the ice-free slopes to the south (right) lead to the Tisenal in Italy. The Iceman site is not located at the lowest part of the ridge (Similaun Lodge), which can only be reached by a man-made path through steep rocks, but rather at a location which can be most easily reached from the south following the natural morphology of the valley. It seems likely that the Iceman took this path, if he approached his final resting place from the south.

forms the border between Austria (to the north) and Italy (to the south). As the hikers approached a shallow ice-filled depression along the ridge at an altitude of 3210 m (near the Tisenjoch), they were startled by seeing the body of a man sticking half-way out from the ice. Unusual climatic conditions in the summer of 1991 (including dust from Sahara resulting in enhanced melting of snow) had partly freed the body from its icy grave. The Iceman was later nicknamed “Ötzi”, after the mountain range

where he was found. Two days after the first discovery, Hans Kammerlander and Reinhold Messner, two famous mountain climbers from South Tyrol, happened to arrive at the site, and the photo of Fig. 2 shows them watching the Iceman, whose lower body is still locked into the ice. From the antiquated equipment found at the site, Messner made a first guess at the age of the man and thought he might have died some 500 years ago. Some of the associated equipment certainly



Fig. 2. The partly freed body of the Iceman as watched by two famous mountain climbers from South Tyrol, Hans Kammerlander (left) and Reinhold Messner (right). Picture taken by K. Fritz (Photo Paul Hanny). Kammerlander holds part of a wooden structure later identified as a carrying support of Ötzi. In the right upper corner the bow can be seen, its lower part stuck in the ice and the upper one leaning against the rocks. Just below the tip of the ski pole held by Messner one can see the smashed remains of a container made of bark from a birch-tree, probably used to carry equipment for making fire.

did not look like belonging to a recently deceased mountain climber. Another two days later (on 23 September 1991) the body was recovered from the ice by Rainer Henn from the Institute of Forensic Medicine at the University of Innsbruck, and was flown to his Institute by helicopter. Next day, when Konrad Spindler from the Institute of Pre- and Protohistory of the University of Innsbruck saw the unusual pieces of equipment found together with the body (in particular the axe with a bronze-like blade), he estimated a very old age (~ 4000 years) of the find. This immediately created great excitement for both scientists and the public, resulting in many “colorful” events in the ensuing weeks.

One important step was the determination of the exact location of the finding place as it was very close to the Austrian–Italian border. According to the Treaty of Saint Germain from 1919 following the end of World War I and the breakup of the Austrian–Hungarian Empire, the border was defined to run along the main watershed of the

Alps, between the north (Inn) and the south (Etsch). Due to thick glacial cover in 1920, the exact location of the watershed could not be determined everywhere, and the border in some places was set only by connecting nearby markers (compare Fig. 1). Some 70 years later, the glaciers had ablated to unprecedentedly low levels and it was commonly presumed that the finding site actually lay within Austrian territory, which is why Austrian authorities were called to the site. After an official survey of the border line, however, it was established that the Iceman had been found 92 m inside Italian territory. According to international regulations, the Iceman therefore belonged to Italy. The irony of this border issue became apparent during the extensive excavation in 1992, when meltwater from the discovery site was actually running off to the north. In any case, the Iceman remained more than 6 years at the University of Innsbruck, from where most of the scientific investigations were organized. In January 1998, Ötzi was brought to his final home at the

newly established South Tyrol Museum of Archaeology (Bolzano, Italy), where he is on display for the public. There he is safely stored in a room kept at glacier-like conditions with a temperature of $-6\text{ }^{\circ}\text{C}$ and a relative humidity of 98%. In addition, an impressive display of his clothing and equipment can be visited.

Popular write-ups of the Iceman story are available in German [1] and in English [2]. The results of scientific investigations of the Iceman are published in a series of monographs [3–6], with the latest one concentrating mainly on paleobotanical results [6].

2. ^{14}C dating of the Iceman

The accelerator mass spectrometry (AMS) laboratories in Zürich and Oxford performed the first ^{14}C measurements on milligram amounts of bone and tissue from the Iceman [7–9]. In Fig. 3 a recalibration of the measured radiocarbon age is plotted [10] using the latest calibration curve [11]. It is apparent that the calibrated date covers a much larger time range than the uncalibrated radiocarbon age, which is obtained directly from the results of the AMS measurements. This is due to the “wiggles” in the calibration curve, which results in a 95.4% (2σ) confidence range of 3370–3100 BC. Nevertheless, the ^{14}C dating result unambiguously established that the Iceman lived before the Bronze Age [2400–800 BC], at the end of the Neolithic period. It also allowed narrowing down the possible Neolithic cultures to the north and to the south of the Alps, from which the Iceman may have originated [12].

The dating of the Iceman clearly shows the current limitation of an absolute age determination with ^{14}C due to the variation in the calibration curve. Why do we need a calibration curve in the first place? This stems simply from the fact that in radiocarbon dating we determine the age from measuring the ^{14}C content today, $^{14}\text{C}_t$, and calculate the age, t , from the exponential decrease of the ^{14}C content with a half-life of $t_{1/2} = 5730$ years:

$$^{14}\text{C}_t = \text{C}_0 e^{-\lambda t} = \text{C}_0 2^{-t/5730}. \quad (1)$$

Here, λ is the decay constant, with a relation to the half-life of $\lambda = (\ln 2)/(t_{1/2})$.

Eq. (1) can be rewritten to give the age as a function of the fraction of ^{14}C left over from the initial amount, C_0 , after time t :

$$\begin{aligned} t &= -(t_{1/2})/(\ln 2) \ln(^{14}\text{C}_t/\text{C}_0) \\ &= -8267 \ln(^{14}\text{C}_t/\text{C}_0) \text{ years.} \end{aligned} \quad (2)$$

In order to obtain t , we have to know the initial ^{14}C content, C_0 . The originator of the ^{14}C dating method, Willard Libby [13], assumed that the cosmic-ray produced ^{14}C content in the atmosphere is constant in time. However, it turned out not to be the case: in Fig. 4 the relative deviation of ^{14}C from a fixed reference value is plotted for the last 40,000 years. The major cause for the variation of ^{14}C are the magnetic fields of the sun and the earth: since cosmic rays (85% protons) are deflected by these fields, which show secular variations in their respective field strengths, the result is a variable production of ^{14}C in the atmosphere. In addition, ^{14}C resides in different reservoirs on earth, with global ^{14}C fractions of $\sim 2\%$ in the atmosphere, $\sim 5\%$ in the biosphere and 93% in the ocean [14]. These ^{14}C reservoirs are coupled together through CO_2 exchange, and varying exchange rates due to major climatic changes can also redistribute older (ocean) and younger ^{14}C , leading to very large changes in $^{14}\text{C}/^{12}\text{C}$ isotope ratios of atmospheric CO_2 [15,16].

It may actually be possible to determine the time period of the Iceman more accurately by dating core samples from the Iceman’s bow and the shaft of the axe. Both are made out of yew, with a narrow tree-ring structure of up to 60 rings within the cross section. Taking samples in well-defined temporal spacings, will allow the application of a procedure called “wigggle matching” [17]. We have submitted a proposal to the Archaeological Museum in Bolzano, Italy, to perform such analyses.

The dependence on a calibration curve, and the fact that ^{14}C is highly variable with time (Fig. 4), is an obstacle for the precision of ^{14}C . It is conceivable – however not yet feasible – to think of an absolute ^{14}C dating method [18] similar to the well-known ^{40}K – ^{40}Ar chronometer. What is required is the measurement of both the parent $^{14}\text{C}_t$, and the decay product $^{14}\text{N}^*$ (the asterisk indicates

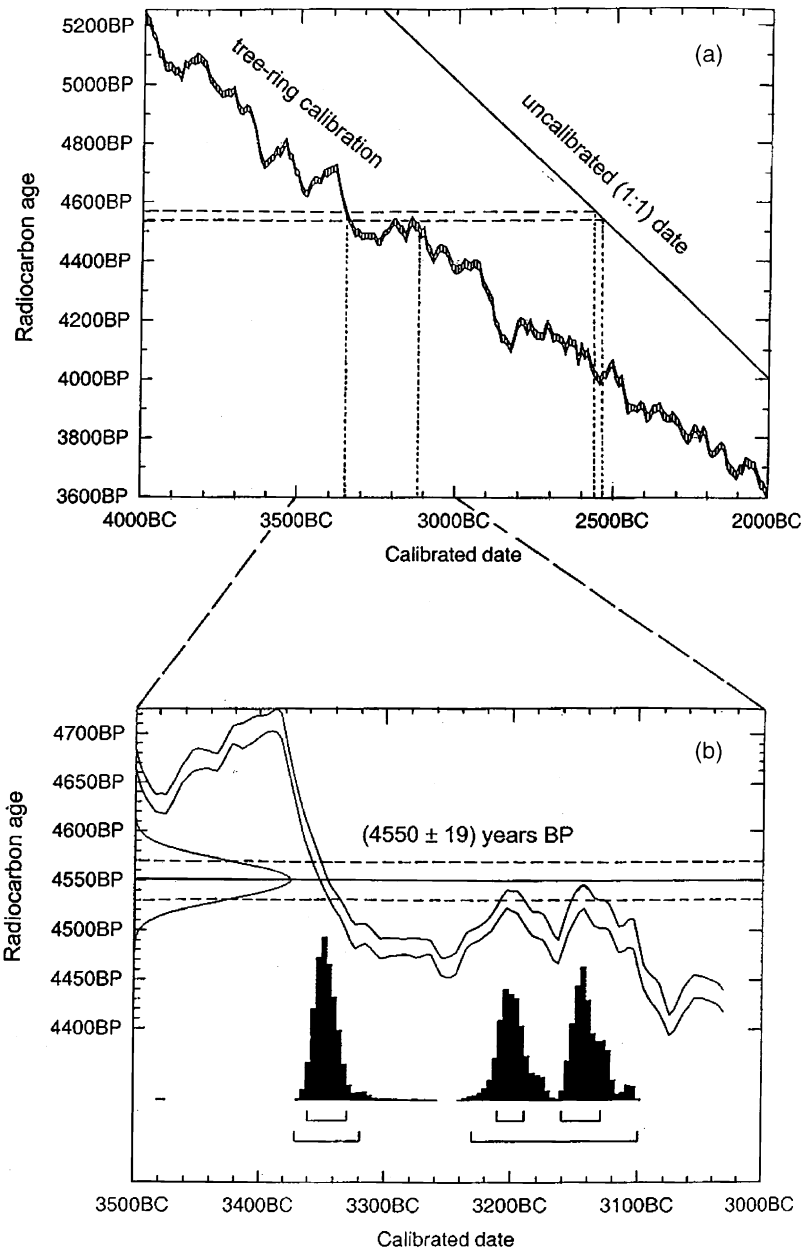


Fig. 3. The determination of the age of the Iceman from ^{14}C measurements at the AMS laboratories of Zürich [7,9] and Oxford [8]. The combined radiocarbon age from these measurements is 4550 ± 19 years BP (before present = 1950 AD). The error is the 68.2% (1σ) confidence value. The uncalibrated age is translated into a calibrated age with the help of the computer program OxCal using the INTCAL98 tree-ring calibration curve [11]. (a) Calibration curve from 4000 to 2000 BC. The straight line at 45° indicates a 1:1 transformation of the radiocarbon age into an uncalibrated calendar date. The intersection of the radiocarbon age with this line and the tree-ring calibration curve shows that the calibrated date is approximately 650 years older. (b) The enlarged “wiggly” section of the calibration curve leads to three different solutions for the calendar date spanning 250 years. The small rectangular brackets beneath the peaks indicate the distribution of the 68.2% (1σ) confidence ranges into three sections of 3360–3300 BC (29.3%), 3210–3190 BC (19.8%) and 3160–3130 BC (19.1%). The large brackets indicate the 95.4% (2σ) confidence ranges of 3370–3320 BC (34.3%) and 3230–3100 BC (61.1%).

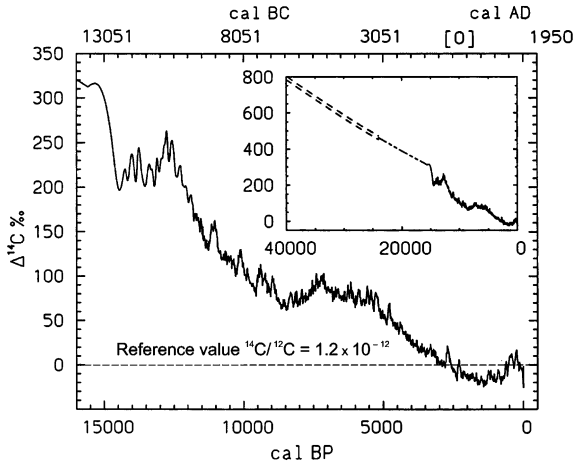


Fig. 4. Relative deviation of the atmospheric ^{14}C content from a fixed reference value. The latter is used to calculate the uncalibrated ^{14}C -age (see Fig. 3). The lower abscissa gives calibrated years BP (before present = 1950), whereas the upper abscissa shows the calendar age in years BC (Before Christ) and AD (Anno Domini). The curve was established by measuring the ^{14}C content in absolutely dated tree rings back to 12,000 years (heavy solid line). Further back in time ^{14}C was measured in corals absolutely dated by the uranium-series method. Beyond 24,000 years, the curve becomes very uncertain (double dashed line in the insert). These results are the basis for the INTCAL98 calibration curve [11], accepted as the official ^{14}C calibration in the Radiocarbon community. Recent results indicate very large deviation of $\Delta^{14}\text{C}$ in the range between 25,000 and 40,000 years ago [15,16].

radiogenic ^{14}N). The radioactive decay of ^{14}C proceeds through



Since C_0 is always $^{14}\text{C}_t + ^{14}\text{N}^*$, we can re-write Eq. (2):

$$\begin{aligned} t &= -(t_{1/2})/(\ln 2) \ln(^{14}\text{C}_t/(C_t + \text{N}^*)) \\ &= 8267 \ln(1 + ^{14}\text{N}^*/^{14}\text{C}_t) \text{ years.} \end{aligned} \quad (2a)$$

We have thus eliminated C_0 and removed one problem, but we introduced another even more formidable problem, i.e. to measure the minute fraction of radiogenic $^{14}\text{N}^*$ in the presence of an ocean of environmental ^{14}N ! It is no surprise that in spite of the obvious importance of an absolute ^{14}C dating method nobody has come up yet with a viable method to actually perform such a measurement. The principle idea is that the low recoil

energy ($E_{\text{max}} = 7.3 \text{ eV}$) of radiogenic $^{14}\text{N}^*$ leads to a certain retention probability of $^{14}\text{N}^*$ in place of the ^{14}C , thus changing the physical and chemical properties of the respective molecule. An even lower recoil energy (2.3 eV) would result for $^{41}\text{K}^*$ in the EC-decay of ^{41}Ca [19]. This 104,000-year radionuclide would be very desirable for radiocalcium dating of bones back to the one-million-year range.

3. ^{14}C dating of materials from the Iceman site

Besides the body of the Iceman itself, a lot of equipment and other material was recovered from the finding place in 1991 [20], apparently belonging to the Iceman as evidenced from ^{14}C dating at the AMS facilities of Uppsala, Gif-sur-Yvette and Vienna [21,22]. The Iceman was found in a shallow depression with only little old ice left at the bottom. Fig. 5 shows a photograph of this place at the end an extensive excavation in 1992 [23], when the depression filled up with meltwater. Continuously draining off meltwater, the finding site was thoroughly searched for materials, removing also the bottom ice layer. Some 500 kg of sediments were collected including botanical and other remains. Some 50 objects were selected and identified by the Institute of Botany of the University of Innsbruck for ^{14}C dating at the VERA facility [24].

During this excavation all the material found was recorded and assigned to a respective spot on the discovery site. A detailed description of the materials and its distribution around the site will be published elsewhere [25]. ^{14}C AMS measurements were performed at the Vienna Environmental Research Accelerator (VERA), a dedicated AMS facility in operation since 1996 [26,27]. Fig. 6 shows the schematic layout of the facility after the recent upgrade to extend VERA for AMS of nuclides of all masses [28]. In its present stage, VERA is probably the most advanced “small” AMS facility anywhere, as it allows one to perform AMS experiments for long-lived radionuclides from ^{10}Be to ^{244}Pu . A summary of all ^{14}C data currently available from the Iceman site is shown in Figs. 7 and 8. The underlying working hypothesis of these measurements was to find evi-



Fig. 5. View of the Iceman finding site at the end of the excavation campaign in 1992 [23]. The site is filled with meltwater, which had been continuously removed during the excavation. On the right side in the middle the rock of the Iceman's final resting place (compare Fig. 2) can be seen. From the shape of the site one can imagine that the Iceman was locked into place by ice not moving anywhere, in contrast to the main glaciers in this area, which rapidly flow downhill (compare Fig. 1). This fortunate circumstances must have contributed to the good state of preservation of the body for thousands of years. (Photo: Amt für Bodendenkmäler, Bozen.)

dence for climatic signatures, which can be compared to available paleoclimate data derived from studying the timberline and glacier snowlines in the Alpine regions [29]. In general, both fauna and flora at the margins of their existence are sensitive proxies for climatic changes. Whereas bast from lime trees and low-altitude grass (Fig. 7) can never grow at this altitude, the high-altitude grass (Fig. 8) can grow there under favorable conditions. Its preferred existence in the period just before the Iceman indicates a warmer climate, consistent with the findings of Patzelt (Fig. 9). Mosses are less sensitive, and can adjust more easily to climatic changes. The wood pieces found at the site indicate human presence. It is interesting to see a piece of charcoal (*Pinus sp./periderme*) at around 4000 BC, probably indicating the presence of humans a 1000 years earlier than the Iceman. This is also supported by the measurement of two soil samples (Fig. 8 bottom) about 100 m away from the Ice-

man site in a rocky niche [30]. The older soil sample shows a thicker layer indicating a warmer climate.

4. Principles of isotopic tracing

Tracing of origin using radiogenic and stable isotopes is routinely applied in the Earth Sciences; see [31] and [32] for comprehensive reviews. *Radiogenic* isotopes are those produced from radioactive decay of natural, long-lived radionuclides such as ^{238}U , ^{235}U , ^{232}Th , ^{87}Rb , ^{147}Sm or ^{176}Lu , which decay to stable ^{206}Pb , ^{207}Pb , ^{208}Pb , ^{87}Sr , ^{143}Nd or ^{176}Hf , respectively, with long half-lives ranging between 0.7 and 106 billion years. In the Earth Sciences, those systems are used for both tracing and dating of rocks. Tracing is possible because parent and daughter elements often exhibit different geochemical behavior. Hence

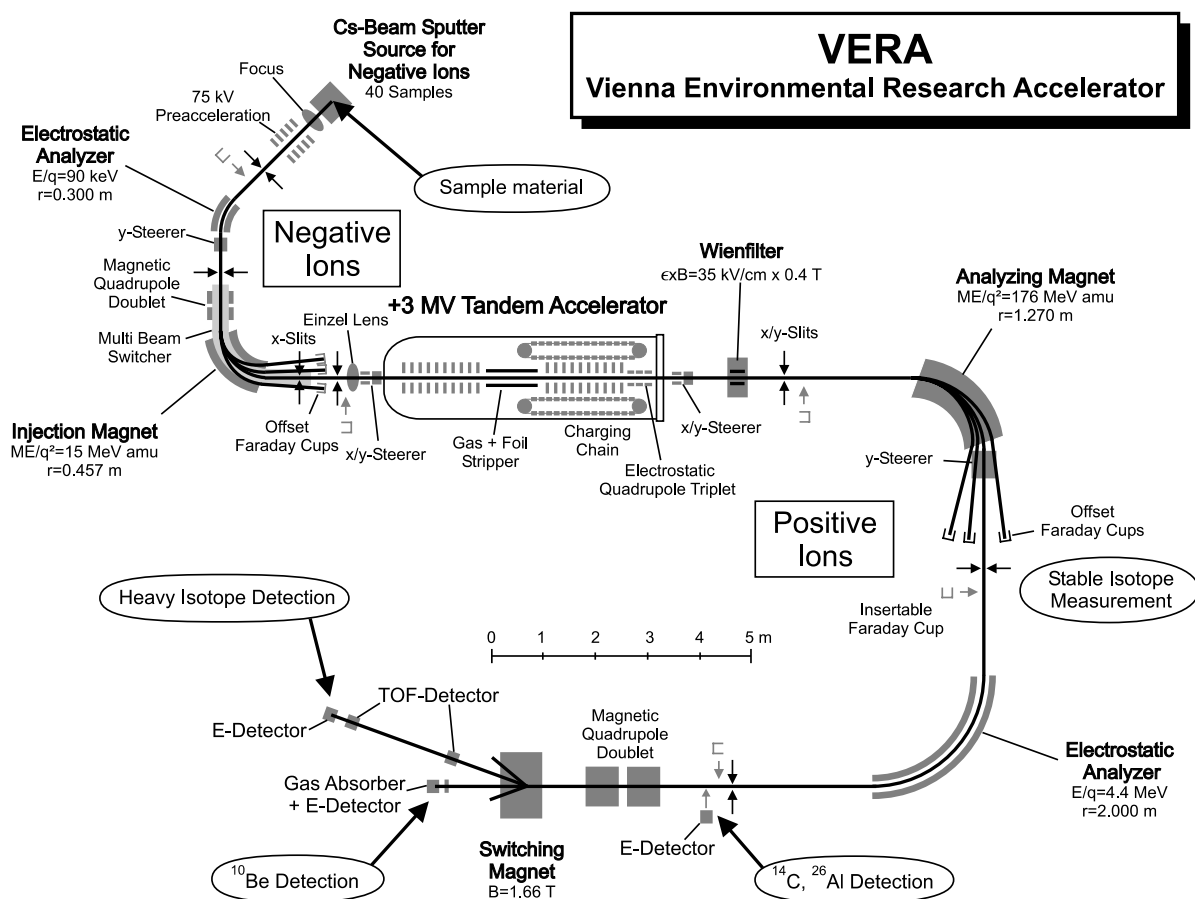


Fig. 6. Schematic layout of the VERA facility after the upgrade for heavy ions [28]. It is based on a 3-MV Pelletron tandem accelerator, and can now be used for AMS experiments ranging from “routine” ^{14}C measurements in the $^{14}\text{C}/^{12}\text{C}$ isotope ratio range from 10^{-12} to 10^{-15} (modern to 50,000 years ago) all the way up the nuclear chart to heavy radionuclides such as ^{182}Hf , ^{210}Pb , ^{236}U and ^{244}Pu [28]. The entire facility can be operated in a fully automated way with remote access through the internet.

parent–daughter elemental ratios (e.g. U/Pb, Rb/Sr, Sm/Nd) vary characteristically amongst the various reservoirs within the Earth (crust, upper mantle, lower mantle, core), and result in distinct isotopic signatures due to different time-integrated radiogenic ingrowth of daughter isotopes (^{206}Pb , ^{207}Pb , ^{87}Sr or ^{143}Nd). The variation in abundance of radiogenic isotopes is often very small, due to the long half-lives involved. Those minute variations are usually expressed as ratios to a non-radiogenic isotope, resulting in e.g. $^{87}\text{Sr}/^{86}\text{Sr}$, $^{206}\text{Pb}/^{204}\text{Pb}$, $^{143}\text{Nd}/^{144}\text{Nd}$ ratios. Isotopic ratios can be analyzed to very high precision in modern multi-collector mass spectrometers (e.g. 0.025‰, 2

standard deviations, for 10^{-8} g of Sr or Nd; [33]). The small variations are often displayed in δ - or ε -notation relative to a standard value:

$$\delta = (\text{ratio}_{\text{sample}}/\text{ratio}_{\text{std}} - 1) \times 10^3,$$

$$\varepsilon = (\text{ratio}_{\text{sample}}/\text{ratio}_{\text{std}} - 1) \times 10^4,$$

where the subscript std refers to standard.

Light elements such as O, C, H, Li, B and others exhibit natural isotopic variations due to their large relative mass differences, induced by physical processes such as evaporation, melting, condensation, or diffusion, and by chemical processes such as photosynthesis, metabolism, to

¹⁴C dating of the Iceman and associated equipment

(all dates are calibrated 2-sigma ranges)

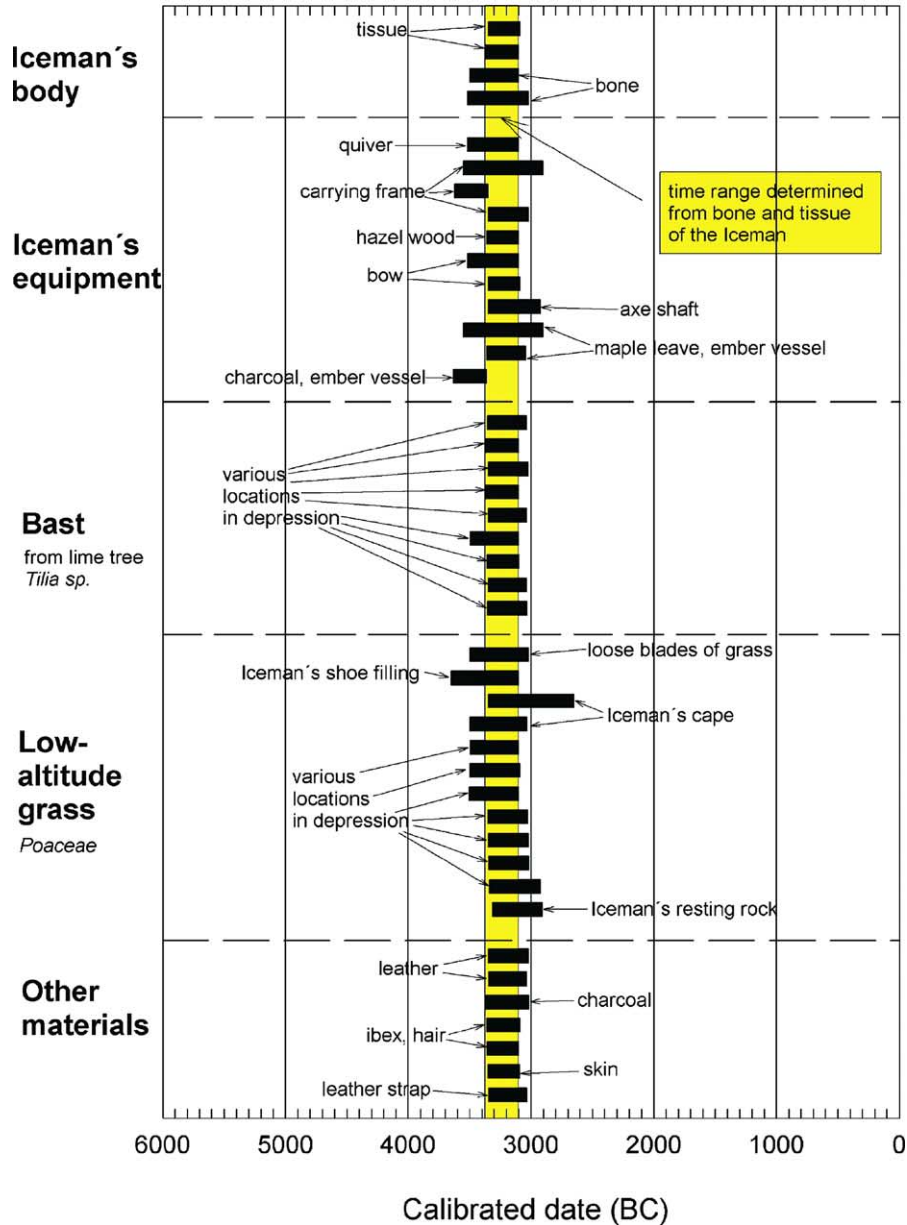


Fig. 7. Summary of ¹⁴C measurements performed on materials, which most likely are directly associated with the Iceman. For all measurements the full 95.4% (2σ) confidence range is given with filled block symbols. The lightly shaded vertical area indicated the average of the four measurements performed on the Iceman's body (compare Fig. 3).

name a few. Such elements are usually referred to as *stable* isotopes. Palaeothermometry with oxygen isotopes [34] is one of the best-known appli-

cations of stable isotopes. The distinction of radiogenic and stable isotopes is somewhat arbitrary since most of the radiogenic isotopes

^{14}C dating for various non-Iceman associated materials

(all dates are calibrated 2-sigma ranges)

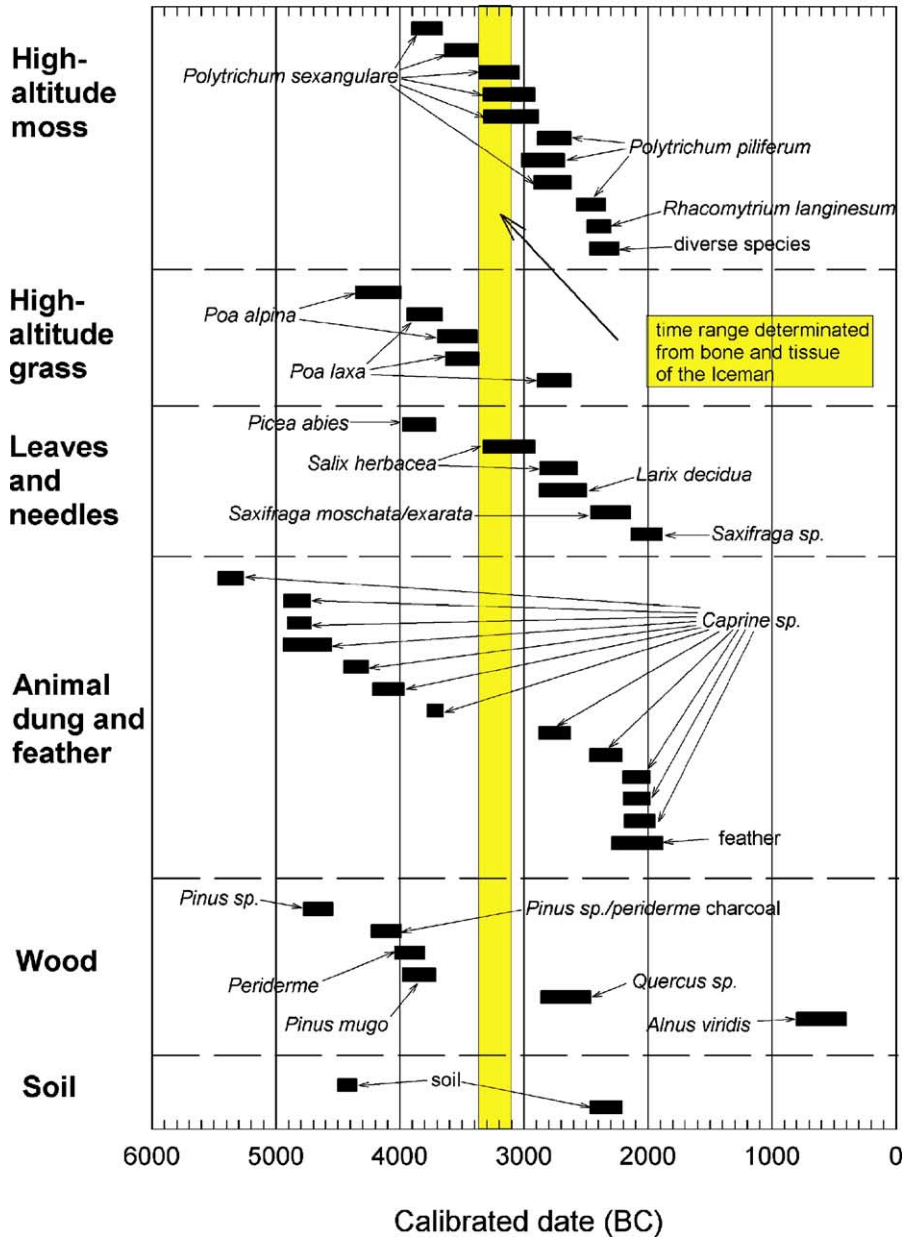


Fig. 8. Summary of ^{14}C measurements which fall outside the range of the Iceman (lightly shaded vertical area). As in Fig. 7, the full 95.4% (2σ) confidence range is given with the filled block symbols. Note that with one exceptions no samples younger than about 2000 years BC have been found.

are stable, too, but common practice in isotope geochemistry. Recently, the advent of a new

mass spectrometric technique called multi-collector inductively-coupled-plasma mass spectrometry

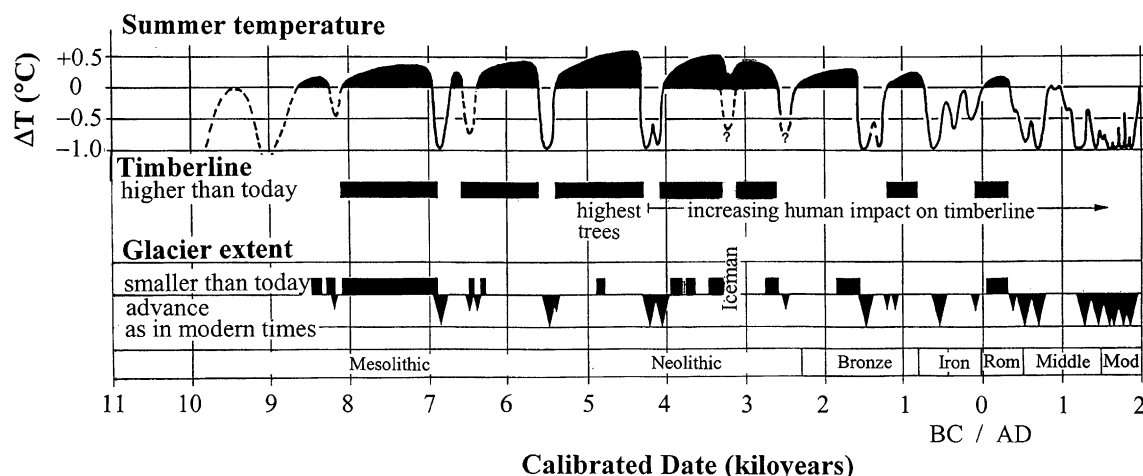


Fig. 9. Schematic Presentation of Alpine climate variations during the last 10,000 years (Holocene), as established by Gernot Patzelt from the Institute of High Mountain Research, University of Innsbruck [29]. The upper curve shows the deviation of the summer temperature (May to September) from the average of 1980–2000; the latter was obtained directly from high-altitude meteorological stations in the Alps. This curve is largely the result of studying the timber line, the glacier snow line, and human activities in high-altitude regions. ^{14}C dating was used to make temporal assignments. The generally warmer climate in the first half of the Holocene, and a cooling trend in the second half is clearly visible.

(MC-ICPMS; e.g. [35]), has enabled the detection of natural isotopic variations also for several heavier elements including Fe, Cu or even Tl [36–38].

5. Tracing of human origin

Radiogenic and stable isotopes provide different information regarding the origin of people, as will be detailed below. In very general terms, radiogenic isotopes (Sr, Pb, Nd) allow the reconstruction of the provenance (origin) of people relative to the local geological environment. Stable isotopes provide information about altitude and position relative to a watershed (O), or paleodiet (C, N).

5.1. Radiogenic isotopes

Via nutrition, humans (and animals) store the isotopic signature of their local geological environment into mineralized hard tissues such as teeth and bones. For the heavy elements Sr, Pb or Nd, no isotopic fractionation has been observed for different positions within the food chain, i.e. soil, plants, herbivores and carnivores. Hence, the iso-

topic signature in hard tissues faithfully records the substrate (soil, bedrock) upon which an individual lived. Different lithologies including their overlying soils exhibit compositional differences and therefore also differ in their respective isotopic signatures, with carbonates, gneisses, granites, or basalts – for example – often showing very characteristic isotopic compositions. This can be illustrated for Sr isotopes, where one isotope, ^{87}Sr , is the product of the decay of ^{87}Rb (Fig. 10). Carbonate sediments usually have very high Sr concentrations, but are essentially devoid of Rb, for which basically no radiogenic ingrowth of ^{87}Sr occurs with time. Unaltered, pure carbonate sediments therefore record the isotopic composition of seawater they precipitated from and have $^{87}\text{Sr}/^{86}\text{Sr}$ ratios between 0.706 and 0.709 [32]. Gneisses and granites are more variable, but generally enriched in Rb versus Sr, for which elevated time-integrated $^{87}\text{Sr}/^{86}\text{Sr}$ ratios of >0.710 occur. Basalts on the other hand usually display $^{87}\text{Sr}/^{86}\text{Sr}$ ratios below 0.706. Generally opposite relationships exist for Nd isotopes in the lithologies mentioned above [32]. Pb isotopes in different lithologies are also highly variable, but less predictable and have therefore to be checked on a case-to-case basis.

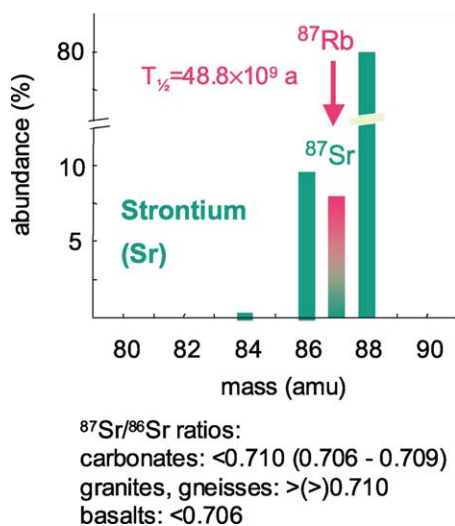


Fig. 10. Schematic diagram of Sr isotopic variations due to β -decay of ^{87}Rb to ^{87}Sr . Depending on Rb/Sr ratio and age, highly variable $^{87}\text{Sr}/^{86}\text{Sr}$ ratios will be the result. The typical values for commonly found rock types are given.

5.2. Stable isotopes

The light elements (e.g. O, C, N) on the other hand, and also some essential transition metals (e.g. Fe [39]) exhibit species-specific fraction in mammal bodies induced by metabolism. In case of oxygen, the isotopic signature stored in biominerals allows the retrieval of the isotopic signature of ingested meteoric water (and indirectly of temperature) due to the species-specific constant fractionation offset [40]. In case of the Iceman, we have utilized differences in the oxygen isotopic composition between water masses in the north and south of the finding side, which coincidentally, but nicely, is exactly located at the main watershed of the Alps. Areas north of the watershed (Austria) mainly derive their precipitation from the northwest, which is isotopically distinct (lighter in $\delta^{18}\text{O}$) to areas south of the finding site, where rain mainly comes from the south (for a review, see [41]). Superimposed onto this global trend is a second phenomenon, because precipitation at higher altitudes is isotopically lighter for oxygen than at lower altitudes [31,42], which can be used to approximately assign an altitude to an isotopic signature retrieved from biominerals.

5.3. Biominerals

The different hard tissues of humans and other mammals mineralize at different ontogenetic stages and incorporate/exchange radiogenic isotopes during these periods. Sr resembles Ca geochemically and is readily incorporated into biominerals composed of Ca-phosphate (apatite); Sr concentrations commonly are around hundred(s) of ppm (weight). Pb and Nd are far less concentrated and occur (far) below the ppm level.

Tooth enamel, even of the permanent dentition, mineralizes during the early childhood, with the first permanent molar being the first tooth to form from birth onwards (for a review, see [43]). Apart from limited passive exchange with the saliva, tooth enamel remains compositionally unchanged after formation. Bones, on the other hand, constantly remineralize and therefore compositionally average the last 10–20 years of life of an individual, dependent on bone type and part of the skeleton. Compact (cortical) bones average over longer periods of time, whereas spongy (cancellous) bone turns over more rapidly [44,45]. Information about the period of Sr turnover in bones can be derived from large-scale ^{90}Sr contaminations following nuclear power plant failures and subsequent careful monitoring of the affected population [46]. Dentine is somewhat transitional, as it has bone-type structure but does not turn over, apart from the formation of small amounts of secondary dentine near the root canal [43].

Post-mortem processes, especially burial in sediments, commonly referred to as diagenesis, can severely affect the trace elemental and isotopic signature of biominerals. Tooth enamel is far less sensitive to later exchange because it has a denser structure and is essentially composed of inorganic apatite with only very little (1%) organic material. Bones, however, have a tubular structure and ~20–30% organic matter, which decomposes after death, leaving spaces for secondary minerals to form [47,48]. Post-mortem alteration of the Iceman is expected to be minor, as he was encased in glacier ice following death, with only limited interaction with melt water being derived from his skin composition [49]. For other human remains found at 'normal' archaeological sites, diagenesis

often limits the use of isotopic techniques as the *in vivo* signature especially of bones has largely been obliterated [48].

6. Tracing the Iceman

We have performed a comprehensive analysis of various materials of the Iceman's body, with the aim to analyze as many as possible materials representing the various ontogenetic stages of his entire life. This extends previous work on bones only [50]. Materials investigated include tooth enamel, dentine, bones (both compact and spongy), intestine wall and intestine content. In addition, a few pieces of his equipment have been analyzed as well. Several ice core samples from the finding site have been used to assess possible post-mortem alteration affecting the trace elemental/isotopic signature of the Iceman samples. Soils from Neolithic–Copper age archaeological horizons, which minimize the risk of picking up an anthropologically modified isotopic signal, crucial in particular for Pb, have been leached with very dilute acetic acid in order to only extract the biologically available trace elemental budget present in a given soil sample. Water samples from several rivers in both northern and southern valleys have been analyzed for their oxygen isotopic composition. They serve as a basis for comparison of the Iceman data, assuming the weather patterns have not grossly changed during the later part of the Holocene. Modern human teeth were chosen for an additional comparison.

A detailed presentation of the material and their isotopic results will be given elsewhere [51] and only a brief summary will be given here.

Radiogenic isotopic compositions of enamel, dentine and bones were determined utilizing three leaching steps for each sample, with sequentially stronger acids to detect possible post-mortem alteration. Any alteration present should be visible in the first leaching step(s), as it comprises the less strongly (crystal-)chemically bound trace elements. Three fragments of Iceman enamel are characterized by similarly high, unaltered $^{87}\text{Sr}/^{86}\text{Sr}$ ratios of 0.7203–0.7214, consistent with compositions of gneisses and schists e.g. close to the finding site.

Sites overlying limestones or widespread Permian volcanic bedrocks further to the south can be excluded as the Iceman's childhood area. Two compact hipbone samples reveal lower $^{87}\text{Sr}/^{86}\text{Sr}$ ratios of 0.7175 and 0.7181, and a spongy bone records a $^{87}\text{Sr}/^{86}\text{Sr}$ ratio of 0.7184 (final leaching steps). Hence, in contrast to the food source during his earliest childhood, the Iceman used food from (and migrated to?) a different region during his last ~1–2 decades of adult life. Fig. 11 depicts preliminary results for $^{87}\text{Sr}/^{86}\text{Sr}$ and $^{206}\text{Pb}/^{204}\text{Pb}$ ratio measurements, demonstrating the power of the method to identify the soil on which the Iceman spent his childhood (enamel analysis), and the later stages of his life (bone analysis).

$\delta^{18}\text{O}$ -analyses of river waters from valleys north and south of the finding site (the latter being located at the main Alpine watershed) have revealed significant differences predominantly between northern and southern rivers, but also in east and west direction. Waters from the southeast of the investigated area (i.e. a $\sim 100 \times 100$ km square with the finding site located close to the middle) display the least depleted $\delta^{18}\text{O}$ values. The preliminary

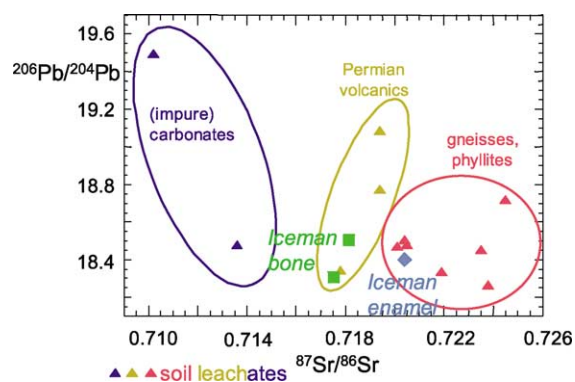


Fig. 11. Preliminary results of $^{206}\text{Pb}/^{204}\text{Pb}$ versus $^{87}\text{Sr}/^{86}\text{Sr}$ isotope ratio measurements of tooth enamel and compact bones of the Iceman, plotted relative to respective data from soils located on various lithologies. The relatively high $^{87}\text{Sr}/^{86}\text{Sr}$ ratios of the Iceman biominerals clearly exclude soils above carbonate rocks for both his child- and adulthood. The results for enamel point towards gneisses/phyllites building up the region for the childhood of the Iceman (e.g. similar to the ones found in the vicinity of the finding site). During his adulthood (represented by the bone value) an isotopically distinct food source was utilized and migration of the Iceman is highly probable, although it is not yet possible to deduce with certainty where to.

$\delta^{18}\text{O}$ analysis of enamel can only be reconciled with waters from the south using the constant oxygen isotope fractionation of human bodies [40], hence excluding a northern origin of the Iceman. This is in stark contrast to conclusions based largely on trace element ratios [50].

The values of meteoric waters calculated to be in equilibrium with $\delta^{18}\text{O}$ values of modern human teeth match those actually measured $\delta^{18}\text{O}$ values of local waters. This adds further confidence to the approach used for interpretation of $\delta^{18}\text{O}$ data in the Iceman's biominerals. Bones are only slightly lighter in $\delta^{18}\text{O}$ when compared to enamel.

7. Conclusion

The present paper attempts to summarize all ^{14}C dating results for the Iceman and his discovery site, to the best of our knowledge. This information may serve as a data base for future investigations about the Iceman and his environment. When this investigation was started, it was hoped to find clear evidence for climatic variations around the time period of the Iceman. Although there are some indications, it is too early to draw definite conclusions. Rather we consider this work as another building block in the complex task to reconstruct the Alpine climate and its variations during the entire Holocene.

In addition, first results on the use of stable and radiogenic isotopes to trace the origin of the Iceman are reported. In our view, it is particularly the combination of several isotopic tracers – here Sr, Pb and O – that allows a better assignment, because a single isotopic tracer rarely yields unequivocal information. The combined Sr, Pb and O isotopic composition of tooth enamel of the Iceman places him to the south of the finding site. However, it cannot be very far south (>50 km from the finding site), since there essentially carbonate bedrocks prevail, which are clearly inconsistent with the very elevated $^{87}\text{Sr}/^{86}\text{Sr}$ ratios in teeth and bones.

It seems certain that the increase in sensitivity and precision of both AMS, TIMS and MC-IC-PMS will deliver isotope information which allow archaeo-forensic studies to trace down such di-

verse things as climate changes during the Holocene, and the detailed origin of a human being from the Neolithic Period. In this case study, all this is centered on the Iceman, one of the most fascinating archaeological finds in recent years.

Acknowledgements

The work presented in this review is the result of very fruitful interactions of the authors with a large number of individuals from a variety of fields. Without claim of completeness we would like to thank G. Bonani, S. Bortenschlager, J.H. Dickson, E. Egarter-Vigl, A. Fleckinger, B. Fowler, H. Fricke, R. Golser, A.N. Halliday, B. Jettmar, A. Lippert, C. Marzoli, M.T. McCulloch, K. Nicolussi, K. Oeggel, G. Patzelt, R. Prinath-Fornwagner, A. Priller, S. Puchegger, W. Rom, H. Seidler, K. Spindler, P. Stadler, P. Steier, U. Tecchiati, P. Tropper, C. Vockenhuber and E.M. Wild.

References

- [1] K. Spindler, *Der Mann im Eis – Neue sensationelle Erkenntnisse über die Mumie aus den Ötztaler Alpen*, Goldmann Verlag, München, 2000, p. 1.
- [2] B. Fowler, *Iceman – Uncovering the Life and Times of a Prehistoric Man Found in an Alpine Glacier*, Random House, New York, 2000, p. 1.
- [3] F. Höpfer, W. Platzer, K. Spindler (Eds.), *Der Mann im Eis – Bericht über das Internationale Symposium 1992 in Innsbruck*, Vol. 1, Veröffentlichungen der Universität Innsbruck Nr. 187, 1992, p. 1.
- [4] K. Spindler, E. Rastbichler-Zissernig, H. Wilfing, D. zur Nedden, H. Nothdurfter (Eds.), *Der Mann im Eis – Neue Funde und Ergebnisse*, Vol. 2, Springer Verlag, Wien, New York, 1995, p. 1.
- [5] K. Spindler, H. Wilfing, E. Rastbichler-Zissernig, D. zur Nedden, H. Nothdurfter (Eds.), *The Man in the Ice – Human Mummies*, Vol. 3, Springer Verlag, Wien, New York, 1996, p. 1.
- [6] S. Bortenschlager, K. Oeggel (Eds.), *The Man in the Ice – The Iceman and his Natural Environment – Paleobotanical Results*, Vol. 4, Springer Verlag, Wien, New York, 2000, p. 1.
- [7] B. Bonani, S. Ivy, T.R. Niklaus, M. Suter, M.A. Housley, C.R. Bronk, G.J. van Klinken, R.E.M. Hedges, in: F. Höpfer, W. Platzer, K. Spindler (Eds.), *Der Mann im Eis – Bericht über das Internationale Symposium 1992 in Innsbruck*, Vol. 1, Publikation der Universität Innsbruck Nr. 187, 1992, p. 108.

- [8] R.E.M. Hedges, R.A. Housley, C.R. Bronk, G.J. van Klinken, *Archaeometry* 34 (2) (1992) 337.
- [9] G. Bonani, S. Ivy, I. Hajdas, T.R. Niklaus, M. Suter, *Radiocarbon* 36 (2) (1994) 247.
- [10] W. Kutschera, W. Rom, *Nucl. Instr. and Meth. B* 164–165 (2000) 12.
- [11] M. Stuiver, P.J. Reimer, E. Bard, J.W. Beck, G.S. Burr, K.A. Hughen, B. Kromer, G. McCormac, J. van der Plicht, M. Spurk, *Radiocarbon* 40 (3) (1998) 1041.
- [12] R. Prinoth-Fornwagner, T.R. Niklaus, *Nucl. Instr. and Meth. B* 92 (1994) 282.
- [13] J. Arnold, W.F. Libby, *Science* 110 (1949) 678.
- [14] Ingeborg Levin, Institut für Umweltp Physik, Universität Heidelberg, private communication.
- [15] Y. Yokoyama, T.M. Esat, L.K. Fifield, *Radiocarbon* 42 (3) 383.
- [16] J.W. Beck, D.A. Richards, R.L. Edwards, B.W. Silverman, P.L. Smart, D.J. Donahue, S. Hererra-Osterheld, G.S. Burr, L. Calsoyas, A.J.T. Jull, D. Biddulph, *Science* 292 (2001) 2453.
- [17] C. Bronk Ramsey, J. van der Plicht, B. Weninger, *Radiocarbon* 43 (2A) (2001) 381.
- [18] J. Szabo, I. Carmi, D. Segal, E. Mintz, *Radiocarbon* 40 (1) (1998) 77.
- [19] W. Kutschera, *AIP Conf. Ser.* 495 (1999) 407.
- [20] A. Lippert, in: F. Höpfel, W. Platzer, K. Spindler (Eds.), *Der Mann im Eis – Bericht über das Internationale Symposium 1992 in Innsbruck*, Vol. 1, Veröffentlichungen der Universität Innsbruck Nr. 187, 1992, p. 245.
- [21] W. Rom, R. Golser, W. Kutschera, A. Priller, P. Steier, E. Wild, *Radiocarbon* 41 (2) (1999) 183.
- [22] W. Kutschera, R. Golser, A. Priller, W. Rom, P. Steier, E. Wild, M. Arnold, N. Tisnerat-Laborde, G. Possnert, S. Bortenschlager, K. Oeggel, in: S. Bortenschlager, K. Oeggel (Eds.), *The Man in the Ice – The Iceman and his Natural Environment*, Vol. 4, Springer Verlag, Wien, New York, 2000, p. 1.
- [23] B. Bagolini, L. Dal Ri, A. Lippert, H. Nothdurfter, in: K. Spindler, E. Rastbichler-Zissernig, H. Wilfing, D. zur Nedden, H. Nothdurfter (Eds.), *Der Mann im Eis – Neue Funde und Ergebnisse*, Vol. 2, Springer Verlag, Wien, New York, 1995, p. 3.
- [24] B. Jettmar, *Radiocarbon Dating at the Discovery Site of the Iceman Ötzi*, Diploma Thesis at the Institut für Isotopenforschung und Kernphysik, Universität Wien, in preparation.
- [25] W. Kutschera, B. Jettmar, S. Bortenschlager, R. Golser, A. Lippert, K. Oeggel, G. Patzelt, A. Priller, S. Puchegger, W. Rom, P. Steier, E.M. Wild, in preparation.
- [26] W. Kutschera, P. Collon, H. Friedmann, R. Golser, P. Hille, A. Priller, W. Rom, P. Steier, S. Tagesen, A. Wallner, E. Wild, G. Winkler, *Nucl. Instr. and Meth. B* 123 (1997) 47.
- [27] A. Priller, R. Golser, P. Hille, W. Kutschera, W. Rom, P. Steier, A. Wallner, E. Wild, *Nucl. Instr. and Meth. B* 123 (1997) 193.
- [28] C. Vockenhuber, I. Ahmad, R. Golser, W. Kutschera, V. Liechtenstein, A. Priller, P. Steier, S. Winkler, *Int. J. Mass Spectrom. Ion Processes* 223&224 (2003) 713.
- [29] G. Patzelt, *Natürliche und anthropogene Umweltveränderungen im Holozän der Alpen*, Rundgespräche der Kommission für Ökologie, Bd. 18 “Entwicklung der Umwelt seit der letzten Eiszeit”, Verlag Dr. Friedrich Pfeil München, 2000, p. 119.
- [30] C. Baroni, G. Orombelli, *Quatern. Res.* 46 (1996) 78.
- [31] G. Faure, *Principles of Isotope Geology*, 2nd Ed., Wiley, New York, 1986, p. 589.
- [32] A.P. Dickin, *Radiogenic Isotope Geology*, Cambridge University Press, 1997, p. 490.
- [33] W. Müller, N.S. Mancktelow, M. Meier, *Earth Planet. Sci. Lett.* 180 (3–4) (2000) 385.
- [34] H.C. Urey, *J. Chem. Soc.* (1947) 562.
- [35] A.N. Halliday, D.-C. Lee, J.N. Christensen, M. Rehkämper, W. Yi, X. Luo, C.M. Hall, C. Ballentine, T. Pettke, C. Stirling, *Geochim. Cosmochim. Acta* 62 (1998) 919.
- [36] C.N. Marechal, P. Telouk, F. Albarede, *Chem. Geol.* 156 (1999) 251.
- [37] A.D. Anbar, J.E. Roe, J. Barling, K.H. Nealson, *Science* 288 (2000) 126.
- [38] M. Rehkämper, M. Frank, J.R. Hein, D. Porcelli, A. Halliday, J. Ingri, V. Liebetrau, *Earth Planet. Sci. Lett.* 197 (1–2) (2002) 65.
- [39] T. Walczyk, F. von Blanckenburg, *Science* 295 (2002) 2065.
- [40] A. Longinelli, *Geochim. Cosmochim. Acta* 48 (1984) 385.
- [41] K. Rozanski, L. Araguas-Araguas, R. Gonfiantini, in: *Climate Change in Continental Isotopic Records*, Geophysical Monograph, 78, American Geophysical Union, Washington, 1993, p. 1.
- [42] U. Siegenthaler, H. Oeschger, *Nature* 285 (1980) 314.
- [43] S. Hillson, *Teeth*, in: *Cambridge Manuals in Archaeology*, Cambridge University Press, 1986, p. 1.
- [44] P. Horn, S. Hölzl, T. Fehr, in: G.A. Wagner, K.W. Beinbauer (Eds.), *Homo heidelbergensis von Mauer: Das Auftreten des Menschen in Europa*, HVA, Heidelberg, 1997, p. 144.
- [45] F.D. Pate, *J. Archaeol. Meth. Theory* 1 (2) (1994) 161.
- [46] E.I. Tolstykh, V.P. Kozheurov, O.V. Vyushkova, M.O. Degteva, *Radiat. Environ. Biophys.* 36 (1997) 25.
- [47] M.J. Kohn, M.J. Schoeninger, W.W. Barker, *Geochim. Cosmochim. Acta* 63 (1999) 2737.
- [48] P. Budd, J. Montgomery, B. Barreiro, R.G. Thomas, *Appl. Geochem.* 15 (2000) 687.
- [49] T.L. Bereuter, W. Mikenda, C. Reiter, *Chem. Eur. J.* 3 (7) (1997) 1032.
- [50] J. Hoogewerff, W. Papesch, M. Karlik, M. Berner, P. Vroon, H. Miesbauer, O. Gaber, K.H. Künzel, J. Kleinjans, *J. Archaeol. Sci.* 28 (9) (2001) 983.
- [51] W. Müller, H. Fricke, A.N. Halliday, M.T. McCulloch, *Isotopic tracing of origin and migration of the Neolithic Alpine Iceman*, in preparation.